The Canadian Mineralogist
Vol. 41, pp. 221-232 (2003)

A RE-EXAMINATION OF THE RARE-EARTH-ELEMENT ORTHOPHOSPHATE STANDARDS IN USE FOR ELECTRON-MICROPROBE ANALYSIS

JOHN J. DONOVAN§

Department of Geological Sciences, The University of Oregon, Eugene, Oregon 97403, U.S.A.

JOHN M. HANCHAR

Department of Earth and Environmental Sciences, The George Washington University, Washington, D.C. 20006, U.S.A.

PHILLIP M. PICOLLI

Department of Geology, The University of Maryland, College Park, Maryland 20742, U.S.A.

MARC D. SCHRIER

Department of Chemistry, The University of California, Berkeley, California 94720, U.S.A.

LYNN A. BOATNER

Solid State Division, Oak Ridge National Laboratory, Oak Ridge, Tennessee 37831, U.S.A.

EUGENE JAROSEWICH

Department of Mineral Sciences, Smithsonian Institution, Washington, D.C. 20560, U.S.A.

ABSTRACT

A re-examination of fourteen standards consisting of orthophosphates of the rare-earth elements, Sc and Y, grown at Oak Ridge National Laboratory in the 1980s and widely distributed by the Smithsonian Institution's Department of Mineral Sciences, reveals that some of the material is significantly contaminated by Pb. The origin of this impurity is the $Pb_2P_2O_7$ flux that is derived from the thermal decomposition of $PbHPO_4$. The lead pyrophosphate flux is used to dissolve the oxide starting materials at elevated temperatures (~1360°C) prior to crystal synthesis. Because these rare-earth-element standards are extremely stable under the electron beam and considered homogeneous, they have been of enormous value to the technique of electron-microprobe analysis (EMPA) whenever samples are to be analyzed for the rare-earth elements, Sc, Y, and P. The monoclinic orthophosphates (monazite structure) show a higher degree of Pb incorporation than the tetragonal orthophosphates (xenotime structure). We here describe the extent of the Pb contamination and explain the degree to which the stoichiometries have been affected by the replacement of *REE* by Pb within the crystal structure.

Keywords: rare-earth elements, *REE*, rare-earth phosphates, orthophosphates, quantitative analysis, electron-probe micro-analysis, standards.

SOMMAIRE

Nous ré-examinons quatorze étalons, des orthophosphates des terres rares, Sc et Y, synthétisés dans les années 80 dans le laboratoire national de Oak Ridge, et distribués à grande échelle par le département des sciences minérales du Smithsonian Institution. Ces matériaux s'avèrent contaminés de façon importante par le plomb. Cette impureté provient de l'utilisation de $Pb_2P_2O_7$ comme fondant, dérivé de la décomposition thermique de $PbHPO_4$. Le pyrophosphate de plomb est utilisé pour dissoudre les matériaux de départ (les oxydes) à température élevée (~1360°C) précédant la synthèse. Parce que ces étalons de terres rares

§ *E-mail address*: donovan@oregon.uoregon.edu

sont très stables sous le faisceau d'électrons, et qu'ils sont considérés homogènes, ils ont eu un impact énorme dans les travaux analytiques portant sur les terres rares, le scandium, l'yttrium et le phosphor faisant appel à la microsonde électronique. Les orthophosphates monocliniques, adoptant la structure de phases du groupe de la monazite, acceptent davantage de plomb dans leur structure que les orthophosphates tétragonaux, adoptant la structure du groupe du xénotime. Nous décrivons le portée de cette contamination, et noux expliquons l'impact de cette impureté sur la stoechiométrie des étalons dû au remplacement des terres rares par le plomb dans la structure cristalline.

(Traduit par la Rédaction)

Mots-clés: terres rares, phosphates de terres rares, orthophosphates, analyse quantitative, microsonde électronique, étalons.

Introduction

The most precise and accurate *in situ* chemical analyses of solid materials that can routinely be achieved on the micrometer scale are made with a modern electron-microprobe analyzer (EMPA). The highest-quality results obtained are generally attributed to the use of carefully designed analytical procedures. These procedures include the use of homogeneous, well-characterized standards with a matrix similar to the unknowns to be analyzed, stable and reliable hardware and electronics, attention to the details of sample preparation (cleanliness, flatness and smoothness of sample surfaces, carbon coat), precise acquisition of X-ray intensities, and proper treatment of the data for instrument drift and matrix corrections.

One of the most critical aspects of this ability to acquire high-quality analytical data is the use of well-characterized and stable standards containing a high concentration of the element in question. For the rare-earth elements (*REE*), this goal has, until recently, been elusive owing to the lack of specimens exhibiting these vital properties. In this contribution, we intend to re-examine an essential tool in the arsenal of the micro-analyst, used for the analysis of samples for the *REE*: the Oak Ridge single-crystal *REE* orthophosphates.

Background Information

The lanthanide orthophosphates, consisting of compounds with the stoichiometry $LnPO_4$, where Ln represents any of the rare-earth elements in the series extending from La to Lu, plus the related compounds YPO_4 and $ScPO_4$, are chemically durable and radiation-resistant refractory materials. During the early 1980s, a variety of single-crystal rare-earth orthophosphate samples were synthesized at Oak Ridge National Laboratory, and their structures were determined from X-ray refinements (Milligan *et al.* 1982, 1983a, b, c, Mullica *et al.* 1985a, b, Boatner 1988, Ni *et al.* 1995). The primary purposes of these studies were varied, but they included evaluations of nuclear and actinide waste disposal and scintillator material research, as well as fundamental characterization of materials. The crystals were synthesized using a high-temperature solvent (flux-growth) technique, the details of which are available in the original papers and the references therein (Boatner & Sales 1988).

Although the starting materials were carefully selected to be free from *REE* impurities, they were grown in a lead pyrophosphate ($Pb_2P_2O_7$) flux. This flux is necessary for growth of large single crystals of these *REE* orthophosphates. The original investigators were not greatly concerned about the presence of Pb in the orthophosphate crystals, since this element was not considered detrimental to their specific applications. However, its presence was detected early on, and the solid-state chemistry of Pb in the orthophosphate was characterized by means of electron paramagnetic resonance spectroscopy, which did confirm that Pb is present, though at an undetermined level (Abraham *et al.* 1980). Subsequently, these materials were investigated for possible use as standards for EMPA by the Smithsonian Institution (Jarosewich & Boatner 1991), and put through a series of tests. These tests evaluated homogeneity and included a comparison with the commonly used *REE* glass standards of Drake & Weill (1972) using the EMPA, and a test for ten selected *REE* trace contaminants (but not Pb) on seven of the compounds using instrumental neutron-activation analysis. Eventually, the materials were shown to be extremely robust under electron bombardment, did not oxidize, were not hygroscopic, and no serious contamination or inhomogeneities were noted at the time. These efforts were followed by a general distribution of the material to interested parties.

In the late 1990s, it was reported to one of us (JJD) that at least one investigator (E.J. Essene, pers. commun.) had noted significant Pb in some of the *REE* phosphate standards. The Pb impurity is especially significant in the $CePO_4$ crystals, whose black color is consistent with possible mixed-valence (Ce^{3+}–Ce^{4+}) effects, the presence of which could alter the high-temperature solid-state chemical properties and lead to an enhanced incorporation of Pb during the crystal-growth process. Subsequent communications to investigators in other laboratories also reported Pb in several of the other materials, with Pb ranging from less than 1 to over 4 wt.% element in the $CePO_4$, depending on the laboratory, and the actual grains analyzed. It is our intent in

this paper to characterize and explain the extent of the Pb contamination noted by these investigators in these otherwise extremely useful standards for EMPA of the *REE*, Sc, Y, and P.

Experimental Methods

Quantitative analyses by wavelength-dispersion spectrometry (WDS) of each of the sixteen orthophosphate samples ($LaPO_4$ USNM 168490; $CePO_4$ USNM 168484; $PrPO_4$ USNM 168493; $NdPO_4$ USNM 168492; $SmPO_4$ USNM 168494; $EuPO_4$ USNM 168487; $GdPO_4$USNM 168488; $TbPO_4$ USNM 168496; $DyPO_4$ USNM 168485; $HoPO_4$ USNM 168489; $ErPO_4$ USNM 168486; $TmPO_4$ USNM 168497; $YbPO_4$ USNM 168498; $LuPO_4$ USNM 168491; $ScPO_4$ USNM 168495; YPO_4 USNM 168499) for 14 *REE* plus Sc, Y, and Pb were done using a Cameca SX–51 electron microprobe at 20 keV, 20 nA , using a beam 10 μm in diameter at the University of California at Berkeley. Included with these materials were a Drake and Weill *REE* glass (Drake & Weill 1972), and two other *REE*-doped glasses discussed in Roeder (1985) and Roeder *et al.* (1987). For quantitative analyses, the *K*α X-ray line was used for Sc, *L*α lines for Y and the other *REE* elements, and the *M*α line was used for Pb. Count times were only 20 seconds on peak and 10 seconds on each off-peak position, owing to the relatively large number of elements to be scanned, except for Pb, where the count times were doubled to 40 and 20 seconds, respectively.

TABLE 1. ANALYTICAL SETUP AND MEASURED ACCURACY FOR QUANTITATIVE ANALYSIS OF SAMPLES FOR THE *REE*

Element	Spectrometer setup	Primary standard	Secondary standard	Difference, % Variance
Sc*K*α	LiF (FPC-2)	$ScPO_4$	-	-
Y*L*α	PET (FPC-1)	YPO_4	YAG (stoichiometric)	+0.368, +0.82%
La*L*α	LiF (FPC-2)	$LaPO_4$	S-254 (1.04% nom.)	-0.020, -1.92%
Ce*L*α	LiF (FPC-2)	$CePO_4$	S-254 (1.04% nom.)	-0.010, -0.95%
Pr*L*α	LiF (FPC-2)	$PrPO_4$	S-254 (1.04% nom.)	-0.103, -9.95%
Nd*L*α	LiF (FPC-2)	$NdPO_4$	S-254 (1.04% nom.)	-0.007, -0.70%
Sm*L*α	LiF (FPC-2)	$SmPO_4$	S-254 (1.04% nom.)	-0.055, -5.27%
Eu*L*α	LiF (FPC-2)	$EuPO_4$	*REE*-1 (3.63% pub.)	+0.069, +1.90%
Gd*L*α	LiF (FPC-2)	$GdPO_4$	*REE*-1 (3.87% pub.)	-0.012, -0.31%
Tb*L*α	LiF (FPC-2)	$TbPO_4$	*REE*-1 (3.78% pub.)	-0.116, -3.08%
Dy*L*α	LiF (FPC-2)	$DyPO_4$	S-254 (1.04% nom.)	-0.035, -3.35%
Ho*L*α	LiF (FPC-2)	$HoPO_4$	S-254 (1.04% nom.)	-0.041, -3.92%
Er*L*α	LiF (FPC-2)	$ErPO_4$	S-254 (1.04% nom.)	-0.047, -4.51%
Tm*L*α	LiF (FPC-2)	$TmPO_4$	*REE*-1 (3.81% pub.)	-0.127, -3.33%
Yb*L*α	LiF (FPC-2)	$YbPO_4$	S-254 (1.04% nom.)	-0.047, -4.53%
Lu*L*α	LiF (FPC-2)	$LuPO_4$	S-254 (1.04% nom.)	-0.103, -9.94%
Pb*M*α	PET (FPC-1)	$PbCO_3$	$PbSiO_3$ (stoichiometric)	+0.550, +0.75%

Note: Analytical spectrometer setup (flow proportional detectors: FPC-1 indicates 1 atm P-10 and FPC-2 indicates 2 atm P-10) for REE elements (and Sc, Y and Pb), results of secondary standard measurements (algebraic difference and percent variance) performed at UC Berkeley. All measurements were made at 20 keV, 20 nA (150 nA for the four grain map in Fig. 5), 10 μm beam diameter, 20 seconds on-peak integration time and 10 seconds on each off-peak, except for Pb, which was counted for 40 seconds on-peak and 20 seconds on each off-peak position (240 seconds on-peak and 120 on each off-peak position for the four grain map in Fig. 5). Each set of analytical results in the table is the average of 10 measurements. For the *REE* elements and Pb, secondary standard accuracy was better than 10% at the 1 wt.% level of concentration in all cases, and better than 6% in all but three cases (Pr, Sm and Lu). All primary standards are synthetic except $PbCO_3$, cerussite from the Tsumeb deposit.

In Table 1, we present a complete description of the analytical setup and the accuracy of the secondary standards for the elements sought (the composition of the *REE* phosphate primary standards in these cases had been previously adjusted for average Pb concentrations). Secondary standards included synthetic yttrium–aluminum garnet (YAG) and alamosite ($PbSiO_3$) from Tsumeb, Namibia. These were assumed to be stoichiometric for Y and Pb, respectively. The Roeder *REE* glass S–254 (Roeder 1985) was assumed to have a nominal concentration (1.04 wt.%) for La, Ce, Pr, Nd, Sm, Dy, Ho, Er, Yb and Lu, and the Drake and Weill *REE*–1 glass was considered to contain published concentrations for Eu, Gd, Tb and Tm (Drake & Weill 1972). In all cases, the accuracy for the secondary standards is better than 10% variance at the 1 to 4% concentration levels and better than 6% variance in all but three cases (Pr, Sm and Lu).

The difficulty in dealing with interfering elements, in analyses of samples containing rare-earth elements using the *L*α X-ray lines, is painfully evident in even cursory WDS spectral scans on these samples and can only be overcome by careful and consistent application of an automatic scheme for correction for all noted spectral interferences. In Table 2, we show the *REE* that interfere with the elements sought. Concentrations of these were quantitatively corrected for using the iteration method of Donovan *et al.* (1993), which is especially well suited for using large-magnitude interferences in trace-element determinations. For the Pb analyses, the *M*α line was used with a quantitative correction for interference by Y (possible high-order interferences from La and Tb were not observed) using YAG as an interference standard. Standard and background intensities along with the calculated P/B (peak to background) value for each line in its associated primary standard are shown in Table 3.

The minimum detection-limits for both single analyses (Scott & Love 1983) and the average of 10 replicate analyses (Goldstein *et al.* 1981) are shown in Table 4. Minimum detection-limits for 10 replicate analyses based on the actual measured standard deviation is about 300–600 ppm for all elements in all matrices, although only values for the $CePO_4$ or $GdPO_4$ matrices are shown in Table 4. A measured detection-limit of 300–600 ppm (0.03–0.06 wt.%) for the average of 10 replicate analyses at 99% confidence was typical in analyses for the *REE* using the previously discussed conditions. The detection limit of Pb at 99% confidence was about 450 ppm (0.045 wt.%).

Analyses of the standards for only Pb, for the purpose of homogeneity tests, were also performed on single grains. These measurements were performed in different areas than those at which the *REE* and Pb measurements done at UC Berkeley, but on the same

sample mount containing all of the primary and secondary standards discussed above for each *REE* orthophosphate. X-ray intensities of Pb were obtained using a JEOL 8900 Superprobe at the University of Maryland at College Park with an accelerating voltage of 20 keV, and a beam current of 150 nA. Count times were 60 seconds on the peak, and 30 seconds for backgrounds

TABLE 2. QUANTITATIVE INTERFERENCES FOR Sc, Y, La, *REE* AND Pb

Element	On-peak interferences
Sc$K\alpha$ at 3.0320	Er$L\beta_2$ (II) at 3.0284
Y$L\alpha$ at 2.6657	La$L\gamma_1$ (III) at 6.4260 (not observed)
La$L\alpha$ at 2.6657	NdLl (I) at 2.6766
Ce$L\alpha$ at 2.5615	
Pr$L\alpha$ at 2.4630	La$L\beta_{1,4}$ (I) at 2.4595, 2.4595 SmLl (I) at 2.4826
Nd$L\alpha$ at 2.3704	Ce$L\beta_{1,4}$ (I) at 2.3566, 2.3499 Pb$L\alpha_{1,2}$ (II) at 2.3504, 2.3732
Sm$L\alpha$ at 2.1998	Ce$L\beta_2$ (I) at 2.2092 Pr$L\beta_3$ (I) at 2.2175 (not observed)
Eu$L\alpha$ at 2.1209	Nd$L\beta_3$ (I) at 2.1273 Pr$L\beta_2$ (I) at 2.1197
Gd$L\alpha$ at 2.0468	Ce$L\gamma_1$ (I) at 2.0489 La$L\gamma_{2,3}$ (I) at 2.0462, 2.0415 Nd$L\beta_2$ (I) at 2.0365
Tb$L\alpha$ at 1.9765	La$L\gamma_4$ (I) at 1.9834 Pr$L\gamma_1$ (I) at 1.9614 (not observed) Sm$L\beta_3$ (I) at 1.9627 (not observed) Pb$L\beta_{1,2}$ (II) at 1.9660, 1.9650 (not observed)
Dy$L\alpha$ at 1.9088	Eu$L\beta_{1,4}$ (I) at 1.9207, 1.9258 YbLl (I) at 1.8946 (possibly observed)
Ho$L\alpha$ at 1.8450	Gd$L\beta_{1,4}$ (I) at 1.8472, 1.8543 LuLl (I) at 1.8362 (not observed)
Er$L\alpha$ at 1.7842	Tb$L\beta_{1,4}$ (I) at 1.7770, 1.7867 Nd$L\gamma_{2,3}$ (I) at 1.8015, 1.7968
Tm$L\alpha$ at 1.7268	Dy$L\beta_{1,4}$ (I) at 1.7110, 1.7212 Gd$L\beta_2$ (I) at 1.7457 Sm$L\gamma_1$ (I) at 1.7275
Yb$L\alpha$ at 1.6718	Eu$L\gamma_1$ (I) at 1.6577 Sm$L\gamma_2$ (I) at 1.6608 Tb$L\beta_2$ (I) at 1.6834 Y$K\alpha_1$ (II) at 1.6580 (possibly observed) Ho$L\beta_4$ (I) at 1.6597 (not observed)
Lu$L\alpha$ at 1.6195	Ho$L\beta_3$ (I) at 1.6207 Dy$L\beta_2$ (I) at 1.6241 Gd$L\gamma_1$ (I) at 1.5928 (possibly observed)
PbMα at 5.2860	Y$L\gamma_3$ (I) at 5.2848 La$L\alpha_1$ (II) at 5.3326 (not observed) Tb$L\beta_1$ (III) at 5.3310 (not observed)

Note: Elements sought and interfering elements quantitatively corrected for using the iteration method of Donovan *et al.* (1991). Many of these interferences are first-order interferences, and therefore have the same energy as the line interfered with. Hence they cannot be reduced by the use of pulse-height analysis (PHA). Selection of alternative (beta) lines is possible in some cases, but the resulting reduction in intensity will also reduce sensitivity. Wavelengths expressed in Å.

TABLE 3. STANDARD PEAK AND BACKGROUND INTENSITIES (LINEAR INTERPOLATION METHOD)

Element	Peak intensity (cps/nA)	Background intensity (cps/nA)	Peak/ Background
Sc$K\alpha$	49.3 ($ScPO_4$)	0.2	246.5
Y$L\alpha$	68.3 (YPO_4)	0.5	136.6
La$L\alpha$	38.5 ($LaPO_4$)	0.3	128.3
Ce$L\alpha$	45.4 ($CePO_4$)	0.5	90.8
Pr$L\alpha$	55.1 ($PrPO_4$)	0.6	91.8
Nd$L\alpha$	64.9 ($NdPO_4$)	0.6	108.1
Sm$L\alpha$	80.8 ($SmPO_4$)	1.3	62.2
Eu$L\alpha$	89.6 ($EuPO_4$)	1.1	81.5
Gd$L\alpha$	95.2 ($GdPO_4$)	1.2	79.3
Tb$L\alpha$	101.9 ($TbPO_4$)	1.3	78.4
Dy$L\alpha$	107.8 ($DyPO_4$)	1.5	71.9
Ho$L\alpha$	113.6 ($HoPO_4$)	2.2	51.6
Er$L\alpha$	119.5 ($ErPO_4$)	2.1	56.9
Tm$L\alpha$	122.9 ($TmPO_4$)	2.5	49.2
Yb$L\alpha$	128.0 ($YbPO_4$)	2.6	49.2
Lu$L\alpha$	131.3 ($LuPO_4$)	3.4	38.6
Pb$M\alpha$	72.0 ($PbCO_3$)	0.6	120.0

Note: Average peak and background intensities measured on the primary standards for the elements sought, along with calculated peak-to-background ratios. Off-peak positions were positioned on the basis of high-resolution spectral scans performed on the low to high off-peak regions of each *REE* plus Pb in each of the *REE* phosphates to avoid off-peak interferences as much as possible.

TABLE 4. DETECTION LIMITS TYPICAL IN A SINGLE ANALYSIS AND AVERAGE IN REPLICATE ANALYSES

Element	Detection limit (point) 0.99 confidence wt.% in $CePO_4$	Detection limit (average of 10) 0.99 confidence wt.% in $CePO_4$
Sc$K\alpha$	0.058	0.018
Y$L\alpha$	0.103	0.024
La$L\alpha$	0.187	0.045
Ce$L\alpha$	0.147 (in $GdPO_4$)	0.050 (in $GdPO_4$)
Pr$L\alpha$	0.104	0.058
Nd$L\alpha$	0.111	0.068
Sm$L\alpha$	0.103	0.042
Eu$L\alpha$	0.137	0.052
Gd$L\alpha$	0.097	0.125*
Tb$L\alpha$	0.139	0.046
Dy$L\alpha$	0.100	0.033
Ho$L\alpha$	0.140	0.042
Er$L\alpha$	0.097	0.042
Tm$L\alpha$	0.139	0.033
Yb$L\alpha$	0.139	0.038
Lu$L\alpha$	0.142	0.043
Pb$M\alpha$	0.077 (in $GdPO_4$)	0.045 (in $GdPO_4$)

* Gd is possibly present as very small, widely dispersed concentrations in the $CePO_4$, which could explain this unusually high calculated detection limit (for example, the calculated average detection limit for Gd$L\alpha$ in $DyPO_4$ is 0.070 wt.%).

Note: the detection limits in a single-point analysis in a matrix of $CePO_4$ at 99% confidence using the method of Love & Scott (1983) (using a $GdPO_4$ matrix for Ce and Pb owing to the fact that Ce is a major element in $CePO_4$ and Pb was determined to be inhomogeneous in the $CePO_4$). Averaged detection-limits for the same matrices at 99% confidence are based on the actual measured standard deviation on 10 points in each standard using the method of Goldstein *et al.* (1981), which assumes a homogeneous sample. Detection limits for the *REE* in a *REE* phosphate matrix for the analytical conditions used was typically 1000–1400 ppm for single-point measurements (Pb was about 800 ppm) and about 300–600 ppm for the average of 10 measurements (Pb was about 450 ppm).

on each side of the peak. The grains were analyzed for Pb using a PETH crystal (which utilizes a smaller-diameter Rowland Circle, allowing for higher count-rates, but has poorer resolution of wavelength), and background positions of +4 mm (L = 173.307 or 5.4013 Å) and –3 mm (L = 166.307 or 5.1828 Å). Cerussite ($PbCO_3$) from Tsumeb, Namibia, was used as a standard for Pb (83.53 wt.% PbO). Although cerussite is a carbonate, it did not appear to degrade under the electron beam during the analyses. The Pb$M\alpha$ X-ray line was used for analyses of all standards, with the exception of YPO_4, where $M\beta$ was used because of an interference from $Y_l\gamma_3$ on Pb$M\alpha$. For these homogeneity measurements of Pb, the *REE* and phosphate concentrations were not actually measured, but were incorporated as stoichiometric proportions into the ZAF algorithm in order to approximately account for atomic number, absorption, and fluorescence matrix-effects. The single-analysis detection limit of Pb at 99% level of confidence under these analytical conditions was about 140 ppm (0.014 wt.% element) based on a standard count-rate of 263.9 cps/nA and a background of 0.8 cps/nA measured on $CePO_4$.

Measurements were done on two different sets of *REE* orthophosphate samples. The first set consists of material for 16 orthophosphates, including those of Sc and Y obtained from one of us (JMH) and mounted along with primary and secondary standards for analysis and interference corrections. These materials were mounted in an acrylic block 25 mm in diameter and approximately 1.5 cm deep using a cold-set epoxy and circulated to both the Berkeley and College Park laboratories. This sample will be referred to as the "Round Robin" mount in the discussion that follows.

The "Round Robin" mount was carefully analyzed for Pb at both Berkeley and College Park to check for inter-laboratory differences since the analytical results on trace-element measurements are extremely sensitive to differences in spectrometer resolution and placement of off-peak positions for the measurements of background intensities. Homogeneity measurements were also done at Berkeley and College Park to check for possible variations in Pb within this material itself.

Additional measurements of Pb concentrations were done on a second set of materials that was originally resident in the standard collection at the UC Berkeley laboratory, to check for possible inter-batch differences in Pb contamination, since some of the material was produced in several runs at Oak Ridge under possibly different conditions of growth. Analyses on this material will be referred to as the "Berkeley" *REE* mount.

Results and Discussion

REE impurities in the orthophosphate standards

Table 5 shows the concentrations of the trace *REE* measured in each of the orthophosphates performed at UC Berkeley on the "Round Robin" mount. As stated in the original paper by Jarosewich & Boatner (1991), the material is generally very pure on the basis of quantitative results using INAA. The only statistically significant *REE* contamination anomalies observed were the presence of approximately 900 ppm of Eu in $GdPO_4$ (Jarosewich & Boatner reported 19 ppm of Eu in $GdPO_4$ using INAA), 1100 ppm of Ho and 700 ppm of Y in the $DyPO_4$ (Jarosewich & Boatner reported 2470 ppm of Ho in $DyPO_4$ using INAA, whereas Y was not sought by INAA), and approximately 1100 ppm of Er in the $TmPO_4$ (Er was not sought by Jarosewich & Boatner with INAA). It is difficult to obtain commercially available *REE* oxide materials that are completely free of other *REE* as impurities owing to the nature of the starting materials (*REE*-rich phosphate and carbonate minerals) that must be processed to extract individual *REE*. The apparent concentration of 0.09 ± 0.07 wt.% Lu in $GdPO_4$ is possibly due to an interference of Gd $L\gamma 1$ at 1.5928 Å, and the 0.06 ± 0.05 wt.% Dy in $YbPO_4$ is possibly due to an interference of YbL_l at 1.8946 Å; finally, the 0.04 ± 0.03 wt.% Yb in YPO_4 is possibly due to an interference of Y$K\alpha_1$ (II) at 1.658 Å. No other interferences could be invoked to explain the other apparent concentrations of *REE* shown in bold in the table.

Pb impurities in the orthophosphate standards

The results for Pb in the last row of Table 5 reveal that Pb is present from almost 2 wt.% down to about 0.5 wt.% element in seven of the *REE* orthophosphates in the "Round Robin" mount (in order of decreasing concentration: $CePO_4$, $LaPO_4$, $SmPO_4$, $PrPO_4$, $NdPO_4$, $EuPO_4$ and $GdPO_4$). The remaining *REE* orthophosphates do not contain Pb concentrations above the UC Berkeley detection limit of 450 ppm. These measurements were averaged from a ten-point traverse on a single grain of each *REE* orthophosphate.

The Pb homogeneity measurements from College Park on the "Round Robin" mount (done on the same single grains but in different locations) show a striking variation in the Pb content in the individual *REE* orthophosphate samples. Figures 1, 2, 3 and 4 are element-concentration maps of the Pb concentrations in wt.% element with the actual positions of the analysis shown as black dots on the maps. Areas with no analysis positions shown are spurious extrapolations beyond the grain-boundary region and should be ignored. In most cases, fragments of broken orthophosphate crystals were used, owing to the nature of the material available, and it was impossible to determine the exact location of the analyses in the crystals (*i.e.*, center or rim). Relative trends across the grains analyzed, however, reveal the magnitude of the variations in Pb content. From these maps, it is also easy to see that seven *REE* orthophosphates contain detectable Pb ($CePO_4$, $LaPO_4$, $SmPO_4$, $PrPO_4$, $NdPO_4$, $EuPO_4$ and $GdPO_4$), and that the variation of Pb within a single grain is generally as large as

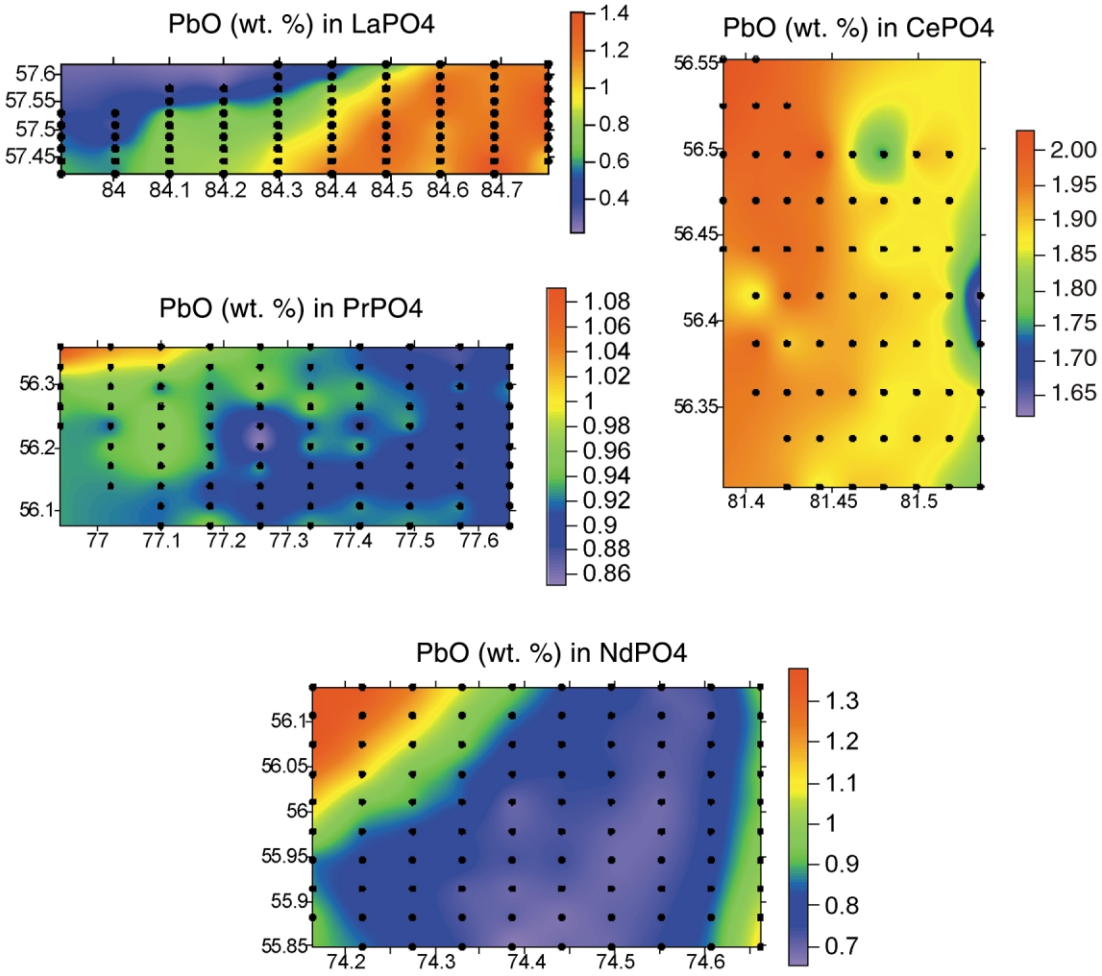

FIG. 1. Quantitative X-ray maps showing the distribution of structurally incorporated lead in four orthophosphate crystals, $LaPO_4$, $CePO_4$, $PrPO_4$ and $NdPO_4$. The amount of Pb is expressed as wt.% PbO (color-coded according according to a vertical scale). X and Y scales (stage coordinates) are expressed in mm.

the concentration itself. It is clear from these maps that the Pb concentrations from a 10-point traverse in a single grain cannot be representative of the average Pb content in the grain. What is even more striking is that the Pb content varies considerably not only within each grain, but even more so from grain to grain, as seen in Figure 5, where Pb maps of four $CePO_4$ grains in the "Berkeley" mount show a tremendous variation among grains, from about 1.5 to 4.5 wt.% element. The numerical averages and standard deviations of the analyses for these four grains are listed in Table 6.

Lead is present in significant amounts only in the monoclinic, high-temperature orthophosphates having the monazite structure ($LaPO_4$ through $GdPO_4$), and is absent, or nearly so, in the tetragonal, xenotime-structure compounds ($TbPO_4$ through $LuPO_4$ and $ScPO_4$ and YPO_4), as can be seen in Figure 6, where Pb concentration is plotted as a function of *REE* atomic number. Boatner & Sales (1988) showed that there is a distinct structural change (monoclinic to tetragonal) between $GdPO_4$ and $TbPO_4$, which suggests that the incorporation of Pb in the monazite structure, and the lack of Pb incorporation in the xenotime-structure orthophosphates, is related to this change in structure. The so-called lanthanide contraction is a continuous decrease in size across the *REE*, and may also play a role in this; however, there are no abrupt decreases in the ionic radii of *REE* trivalent across the series (including from Gd to Tb). Our data suggest that the inclusion of the large divalent lead (*e.g.*, 1.29 Å in eight-fold coordination: Sh-

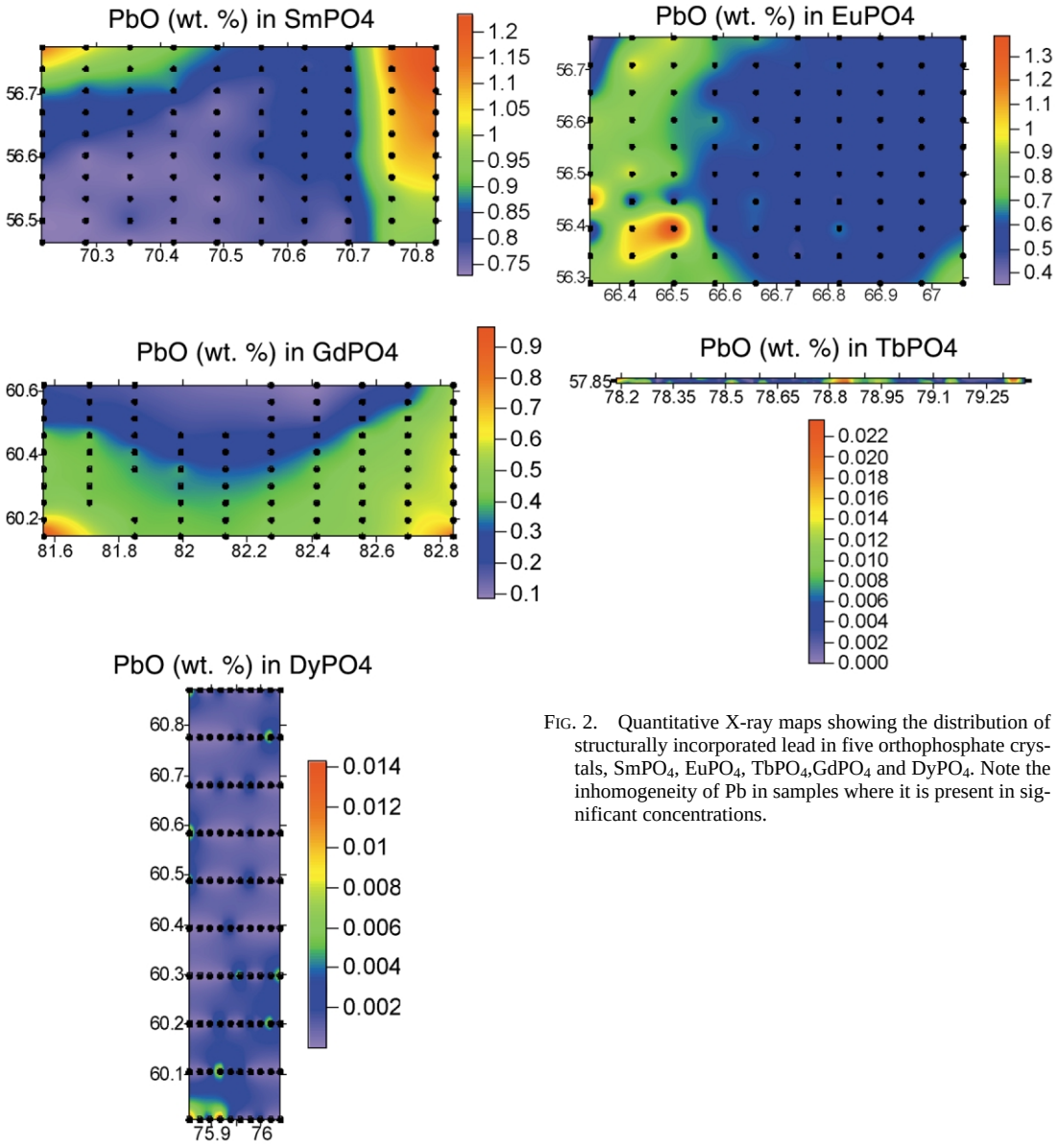

FIG. 2. Quantitative X-ray maps showing the distribution of structurally incorporated lead in five orthophosphate crystals, $SmPO_4$, $EuPO_4$, $TbPO_4$,$GdPO_4$ and $DyPO_4$. Note the inhomogeneity of Pb in samples where it is present in significant concentrations.

annon 1976) ion is limited by the space available in the heavy *REE*–O_8 (*HREE*O_8) polyhedra, and that the divalent Pb ion will not fit easily into the xenotime structure (Ni *et al.* 1995). For the monoclinic orthophosphates, the light *REE*–O_9 (*LREE*O_9) polyhedron is much larger and can accommodate the divalent Pb^{2+} ion into the monazite structure (Ni *et al.* 1995).

In examining the *REE*PO_4 structures, it is evident that when the *REE* cation radius contracts beyond a certain point (empirically, 1.05 Å), the *REE* cation becomes too small to maintain the monoclinic structure-type, and the structure distorts to a lower-density, lower-energy, tetragonal structure-type. Once this change from monoclinic to tetragonal symmetry has occurred, the divalent lead cation can no longer fit into such confined *HREE*O_8 polyhedra. The tetragonal orthophosphates are all of the same structure-type, with a slight contraction of unit-cell volume with increasing atomic number. The same

holds true for the monoclinic orthophosphates. There is a dramatic jump in the cell volumes between Gd (276 $Å^3$) and Tb (292 $Å^3$) with the phase change.

The tetravalent lead cation, with an ionic radius of 0.94 Å (Shannon 1976), would appear to fit better into the tetragonal xenotime-structure orthophosphates with the smaller *HREE* cations (1.04 to 0.87 Å: Shannon 1976), but significant Pb was not observed in those samples. Abraham *et al.* (1980) did find some trivalent Pb in their EPR experiments, but other valence states of Pb such as tetravalent lead could have been present since they are not observable by means of EPR spectroscopy (Abraham *et al.* 1980). The flux used for crystal growth, $Pb_2P_2O_7$, derived from the decomposition of $PbHPO_4$, contains divalent lead; thus it seems more likely that the Pb was in the divalent state under the conditions of synthesis.

Characterizing the exact extent of Pb contamination within a given orthophosphate is problematic because of the degree to which the Pb concentrations vary, not

TABLE 5. TRACE Pb AND *REE* CONCENTRATIONS IN THE *REE*PO_4 STANDARDS

	$ScPO_4$	YPO_4	$LaPO_4$	$CePO_4$	$PrPO_4$	$NdPO_4$	$SmPO_4$	$EuPO_4$
Sc$K\alpha$	-	0.01 ± 0.01	0.01 ± 0.02	0.01 ± 0.01	0.01 ± 0.01	0.01 ± 0.01	0.01 ± 0.01	0.00 ± 0.00
Y$L\alpha$	0.01 ± 0.02	-	0.01 ± 0.01	0.01 ± 0.01	0.00 ± 0.01	0.02 ± 0.03	0.01 ± 0.02	0.00 ± 0.00
La$L\alpha$	0.01 ± 0.01	0.02 ± 0.03	-	0.00 ± 0.00	0.03 ± 0.05	0.02 ± 0.04	0.03 ± 0.03	0.01 ± 0.01
Ce$L\alpha$	0.00 ± 0.01	0.05 ± 0.06	0.01 ± 0.01	-	0.03 ± 0.04	0.03 ± 0.04	0.03 ± 0.04	0.02 ± 0.02
Pr$L\alpha$	0.03 ± 0.03	0.01 ± 0.02	0.07 ± 0.13*	0.02 ± 0.03	-	0.00 ± 0.01	0.01 ± 0.01	0.02 ± 0.03
Nd$L\alpha$	0.00 ± 0.00	0.01 ± 0.02	0.00 ± 0.01	0.01 ± 0.02	0.01 ± 0.03	-	0.00 ± 0.01	0.04 ± 0.04
Sm$L\alpha$	0.02 ± 0.03	0.01 ± 0.02	0.01 ± 0.02	0.02 ± 0.04	0.01 ± 0.02	0.00 ± 0.00	-	0.01 ± 0.02
Eu$L\alpha$	0.02 ± 0.03	0.01 ± 0.02	0.03 ± 0.03	0.00 ± 0.01	0.08 ± 0.11*	0.03 ± 0.05	0.03 ± 0.02	-
Gd$L\alpha$	0.02 ± 0.03	0.02 ± 0.03	0.03 ± 0.06	0.04 ± 0.05	0.01 ± 0.03	0.02 ± 0.03	0.00 ± 0.00	0.02 ± 0.05
Tb$L\alpha$	0.01 ± 0.01	0.02 ± 0.03	0.02 ± 0.03	0.00 ± 0.01	0.03 ± 0.04	0.00 ± 0.00	0.03 ± 0.05	0.00 ± 0.01
Dy$L\alpha$	0.03 ± 0.02	0.02 ± 0.02	0.03 ± 0.04	0.02 ± 0.03	0.00 ± 0.00	0.00 ± 0.00	0.00 ± 0.00	0.02 ± 0.03
Ho$L\alpha$	0.01 ± 0.02	0.01 ± 0.02	0.02 ± 0.03	0.02 ± 0.03	0.00 ± 0.00	0.00 ± 0.01	0.00 ± 0.00	0.00 ± 0.00
Er$L\alpha$	0.03 ± 0.03	0.02 ± 0.02	0.02 ± 0.03	0.03 ± 0.04	0.00 ± 0.00	0.02 ± 0.03	0.07 ± 0.04	0.00 ± 0.00
Tm$L\alpha$	0.02 ± 0.02	0.01 ± 0.02	0.02 ± 0.02	0.01 ± 0.02	0.02 ± 0.03	0.02 ± 0.02	0.06 ± 0.07	0.06 ± 0.06
Yb$L\alpha$	0.00 ± 0.00	0.03 ± 0.04	0.02 ± 0.03	0.04 ± 0.05	0.04 ± 0.04	0.03 ± 0.03	0.02 ± 0.03	0.02 ± 0.03
Lu$L\alpha$	0.02 ± 0.03	0.01 ± 0.03	0.01 ± 0.02	0.03 ± 0.04	0.02 ± 0.03	0.04 ± 0.03	0.00 ± 0.00	0.00 ± 0.01
Pb$M\alpha$	**0.00 ± 0.00**	**0.01 ± 0.01**	**1.05 ± 0.17**	**1.68 ± 0.07**	**0.77 ± 0.04**	**0.60 ± 0.03**	**0.99 ± 0.07**	**0.52 ± 0.06**

	$GdPO_4$	$TbPO_4$	$DyPO_4$	$HoPO_4$	$ErPO_4$	$TmPO_4$	$YbPO_4$	$LuPO_4$
Sc$K\alpha$	0.01 ± 0.01	0.00 ± 0.00	0.01 ± 0.01	0.01 ± 0.02	0.01 ± 0.02	0.00 ± 0.00	0.00 ± 0.01	0.01 ± 0.02
Y$L\alpha$	0.01 ± 0.02	0.01 ± 0.02	**0.07 ± 0.05**	0.02 ± 0.03	0.02 ± 0.03	0.01 ± 0.01	0.04 ± 0.03	0.03 ± 0.03
La$L\alpha$	0.02 ± 0.04	0.01 ± 0.02	0.02 ± 0.04	0.03 ± 0.04	0.01 ± 0.02	0.01 ± 0.01	0.03 ± 0.05	0.02 ± 0.03
Ce$L\alpha$	0.03 ± 0.04	0.01 ± 0.02	0.02 ± 0.02	0.01 ± 0.03	0.03 ± 0.04	0.01 ± 0.01	0.01 ± 0.02	0.01 ± 0.02
Pr$L\alpha$	0.01 ± 0.02	0.01 ± 0.03	0.01 ± 0.02	0.02 ± 0.03	0.02 ± 0.04	0.01 ± 0.03	0.02 ± 0.05	0.01 ± 0.02
Nd$L\alpha$	0.01 ± 0.02	0.02 ± 0.03	0.01 ± 0.02	0.01 ± 0.03	0.02 ± 0.04	0.03 ± 0.04	0.00 ± 0.00	0.03 ± 0.04
Sm$L\alpha$	0.02 ± 0.03	0.00 ± 0.01	0.03 ± 0.04	0.00 ± 0.01	0.02 ± 0.02	0.03 ± 0.03	0.03 ± 0.03	0.02 ± 0.03
Eu$L\alpha$	0.09 ± 0.06	0.03 ± 0.03	0.00 ± 0.01	0.00 ± 0.01	0.01 ± 0.03	0.01 ± 0.01	0.01 ± 0.02	0.01 ± 0.01
Gd$L\alpha$	-	0.01 ± 0.02	0.01 ± 0.02	0.00 ± 0.01	0.00 ± 0.00	0.02 ± 0.02	0.02 ± 0.03	0.01 ± 0.01
Tb$L\alpha$	0.01 ± 0.02	-	0.02 ± 0.03	0.01 ± 0.01	0.00 ± 0.00	0.02 ± 0.03	0.02 ± 0.03	0.01 ± 0.03
Dy$L\alpha$	0.00 ± 0.00	0.00 ± 0.00	-	0.00 ± 0.00	0.02 ± 0.04	0.00 ± 0.00	0.06 ± 0.05	0.01 ± 0.03
Ho$L\alpha$	0.14 ± 0.21*	0.01 ± 0.02	**0.11 ± 0.06**	-	0.01 ± 0.01	0.01 ± 0.03	0.02 ± 0.04	0.03 ± 0.03
Er$L\alpha$	0.00 ± 0.00	0.05 ± 0.09	0.01 ± 0.02	0.00 ± 0.00	-	**0.11 ± 0.07**	0.02 ± 0.02	0.00 ± 0.01
Tm$L\alpha$	0.01 ± 0.02	0.00 ± 0.00	0.03 ± 0.05	0.03 ± 0.03	0.00 ± 0.00	-	0.00 ± 0.01	0.04 ± 0.04
Yb$L\alpha$	0.01 ± 0.01	0.02 ± 0.03	0.00 ± 0.01	0.00 ± 0.00	0.03 ± 0.04	0.00 ± 0.00	-	0.00 ± 0.00
Lu$L\alpha$	0.09 ± 0.07	0.02 ± 0.03	0.02 ± 0.05	0.05 ± 0.07	0.00 ± 0.00	0.01 ± 0.04	0.00 ± 0.00	-
Pb$M\alpha$	**0.49 ± 0.07**	**0.02 ± 0.02**	**0.02 ± 0.03**	**0.02 ± 0.03**	**0.02 ± 0.02**	**0.01 ± 0.02**	**0.02 ± 0.03**	**0.04 ± 0.04**

* Large-magnitude interference corrections, resulting in some loss of precision at trace levels. The apparent concentrations and large standard deviations for these three cases could be greatly reduced by using longer acquisition times on the unknown and the standard for the interference correction.

Note: Average trace concentration of *REE* plus Sc, Y and Pb (in wt.%) for the USNM *REE* phosphates in the "Round Robin" mount. The quoted uncertainty is the measured 1σ value for 10 measurements. The only statistically significant *REE* contamination anomalies noted were the possible presence of Eu in the $GdPO_4$, Y and Ho in the $DyPO_4$, and Er in the $TmPO_4$ standards.

The apparent concentration of 0.09 ± 0.07% Lu in $GdPO_4$ is possibly due to an interference of Gd$L\gamma_1$ at 1.5928 Å and the 0.06 ± 0.05% of Dy in $YbPO_4$ is possibly due to an interference of YbL_η at 1.8946 Å, and finally the 0.04 ± 0.03% of Yb in YPO_4 is possibly due to an interference of Y$K\alpha_1$ (II) at 1.658 Å. No other interferences could be invoked to explain the other apparent concentrations of *REE* shown in bold. Pb was a significant contaminant in seven of the *REE*PO_4 samples, specifically (in order of decreasing concentration): $CePO_4$, $LaPO_4$, $SmPO_4$, $PrPO_4$, $NdPO_4$, $EuPO_4$ and $GdPO_4$.

only within a single grain but also from grain to grain. For this reason, we recommend that each laboratory perform systematic X-ray mapping for Pb of their "in house" *REE* orthophosphate grains to determine the actual extent and variation of Pb contamination in their own mounts. As seen in Figure 5 (*e.g.*, grain #3), it may be that the Pb contamination in one or another of the grains is sufficiently homogeneous to still be suitable for use as a quantitative standard for major-element concentrations of the *REE* in question. Once the Pb concentration for a homogeneous grain is known and the position noted, the measured amount of Pb can be proportionally subtracted from the theoretical *REE*PO_4 composition and entered into the laboratory's standard compositional database for general use.

Implications for EMPA dating of minerals based on U/Pb concentrations

For EMPA dating of minerals with monazite or xenotime compositions, the modified stoichiometries of the orthophosphates will generally not affect quantitative results beyond the analytical sensitivity of most measurements. Using EMPA, a natural crystal of monazite-(Ce) from the Geological Survey of Canada collection (R. Stern, pers. commun.) was analyzed in this study using the orthophosphate standards. A stoichiometric composition of the *REE*PO_4 compounds was assumed, as well as the actual composition of the *REE*PO_4 compounds using the Pb concentrations determined in this study (*i.e.*, $REE_{1-x}Pb_xPO_4$). We determined that the uncertainties from counting statistics (primarily from Pb owing to its low abundance in natural monazite-group minerals) exceeded any uncertainties introduced from the Pb substituting for the *REE* in the orthophosphates in the ZAF routine used to calculate the U, Th, and Pb concentrations. In addition, the EMPA ages (Montel *et al.* 1996) determined in this comparison were within the error of the measurements using the stoichiometric composition of monazite-(Ce), and actual compositions of the monazite-(Ce) with and without correction for the Pb impurities determined in this study.

For trace-element analyses of accessory minerals rich in light *REE* (*LREE*) and middle *REE* (*MREE*), such as monazite- and apatite-group minerals, or *LREE*- or *MREE*-rich synthetic materials, care should be taken to determine the effect of the Pb nonstoichiometry in the specific orthophosphate standards used in the electron-microprobe laboratory, and corrections should be made in the software for the actual composition of the standards in order to minimize any losses in accuracy due to the Pb impurities in the standards. Although the effect of the Pb impurities does not seem to play a large role in determining trace-element concentrations, our datasets are limited and based on only these analyzed samples. Operators of each laboratory should determine the Pb content in each of their orthophosphate standards. For EMPA analyses of minerals that contain the *HREE*, Y, or Sc, such as zircon, pretulite or xenotime, the extremely small concentrations of Pb in these orthophosphate standards will have a negligible effect on the measured *REE* concentrations in the unknowns.

Regarding which *REE*PO_4 material should be used for P as an EMPA standard, we suggest that one of the tetragonal orthophosphates should be used to minimize any nonstoichiometry introduced by Pb impurities.

Pb in natural monazite versus natural xenotime

In comparing U/Pb values of natural monazite and xenotime from the literature (*e.g.*, Parrish 1990), it appears that natural crystals of monazite contain more common (*i.e.*, nonradiogenic) Pb than natural xenotime (*e.g.*, few parts per million of common Pb in monazite and less than 100 parts per billion common Pb in xenotime). In part, this observation is biased owing to a weighted dataset with far fewer data on xenotime than on monazite. This is also probably partly attributable to analytical problems associated with preparing the samples and analyzing monazite or xenotime grains that may contain inclusions of any minerals (*e.g.*, feldspar) with a greater affinity for Pb than either monazite or xenotime, which makes comparison of published analytical results difficult.

CONCLUSIONS

Owing to their qualities of robustness under the electron beam, resistance to oxidation, and *REE* purity, the *REE* orthophosphate standards remain a valuable set of standards for EMPA despite significant Pb contamination in at least seven of the sixteen samples we examined. Of those with measurable amounts of Pb contamination, only the monoclinic $CePO_4$, and possibly the $LaPO_4$, and $SmPO_4$, contain enough Pb to noticeably affect the stoichiometry of the material for use as a primary standard for major-element quantitative analysis (approximately 2 to 4% variance from their theoretical compositions). None of the tetragonal, xenotime-structure orthophosphates ($GdPO_4$ to $LuPO_4$, $ScPO_4$ and YPO_4) contain appreciable Pb.

TABLE 6. GRAIN-TO-GRAIN VARIATION IN Pb (wt.%) WITHIN THE $CePO_4$ MATERIAL IN THE "BERKELEY" *REE* MOUNT

	Average	Standard deviation	Minimum	Maximum
Grain #1	2.68 %	0.45 %	2.04 %	3.47 %
Grain #2	2.55	0.16	2.33	2.83
Grain #3	1.54	0.04	1.48	1.59
Grain #4	3.64	0.46	3.08	4.50

Note: average wt.% Pb and standard deviation of four grains from the "Berkeley" mount mapped in Figure 5 in elemental weight percent. Analytical conditions were 20 keV, 150 nA and a beam 10 μm in diameter. Each analysis is the average of 13 to 16 measurements distributed over the face of each grain.

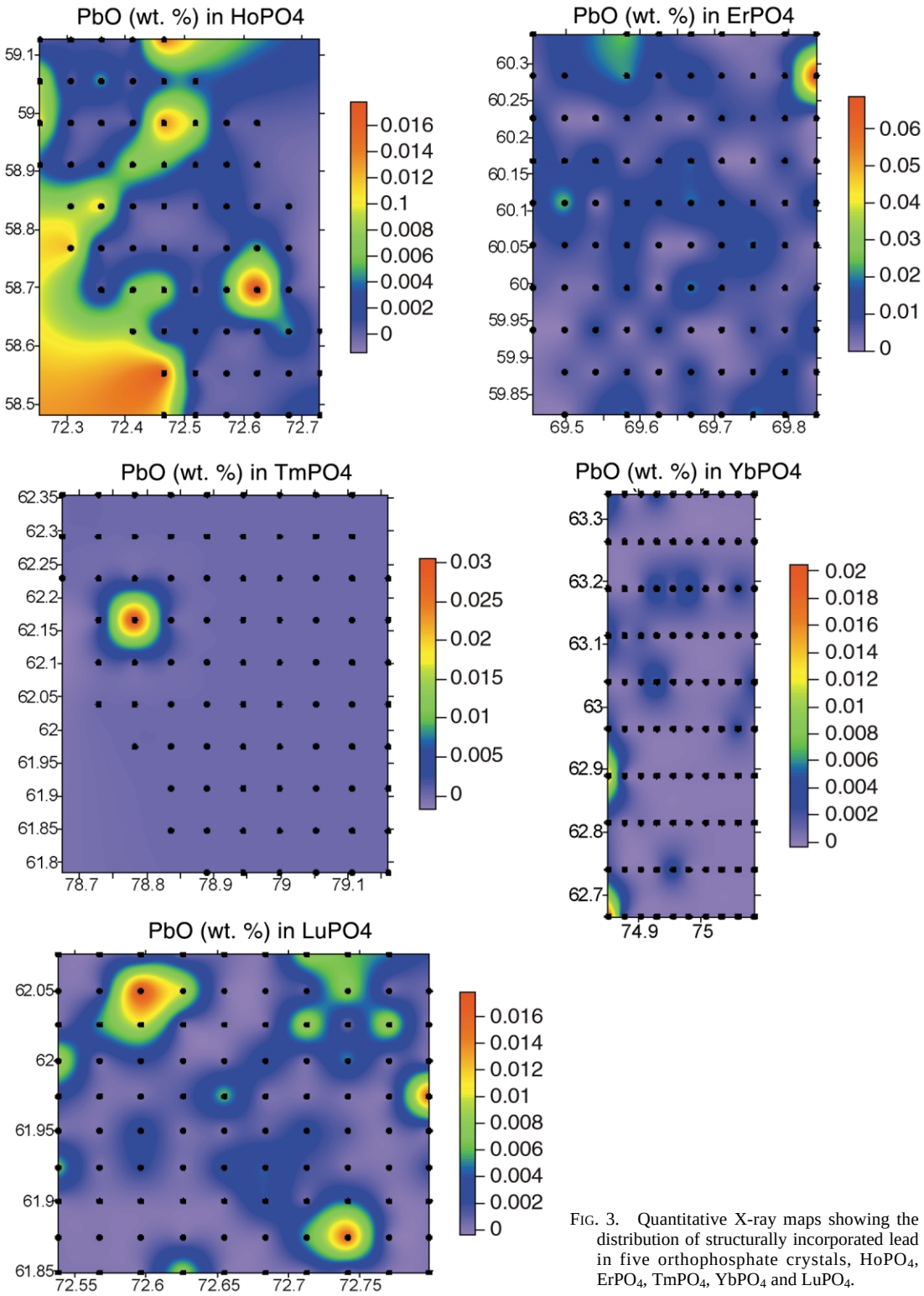

FIG. 3. Quantitative X-ray maps showing the distribution of structurally incorporated lead in five orthophosphate crystals, $HoPO_4$, $ErPO_4$, $TmPO_4$, $YbPO_4$ and $LuPO_4$.

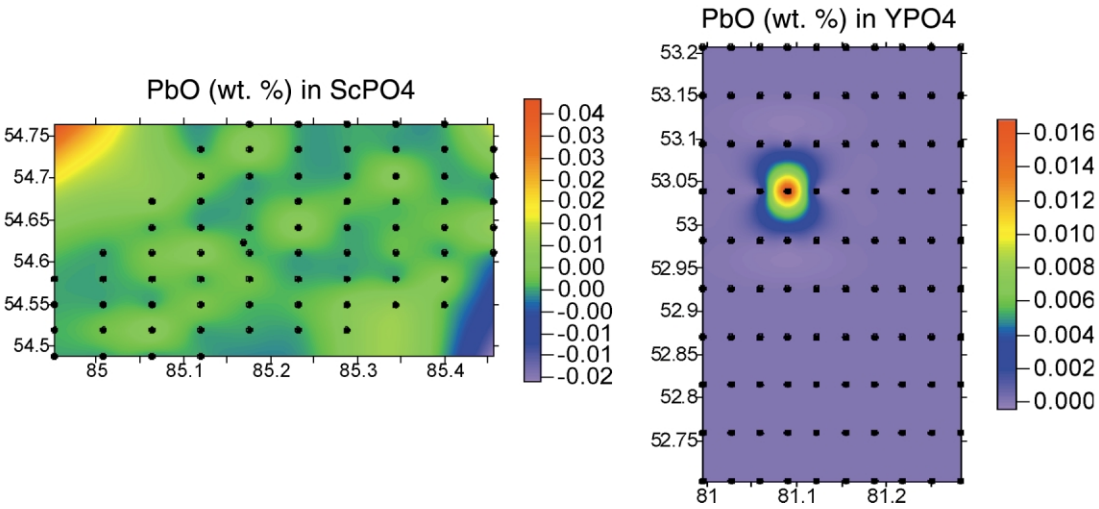

FIG. 4. Quantitative X-ray maps showing the distribution of structurally incorporated lead in two orthophosphate crystals, $ScPO_4$ and YPO_4.

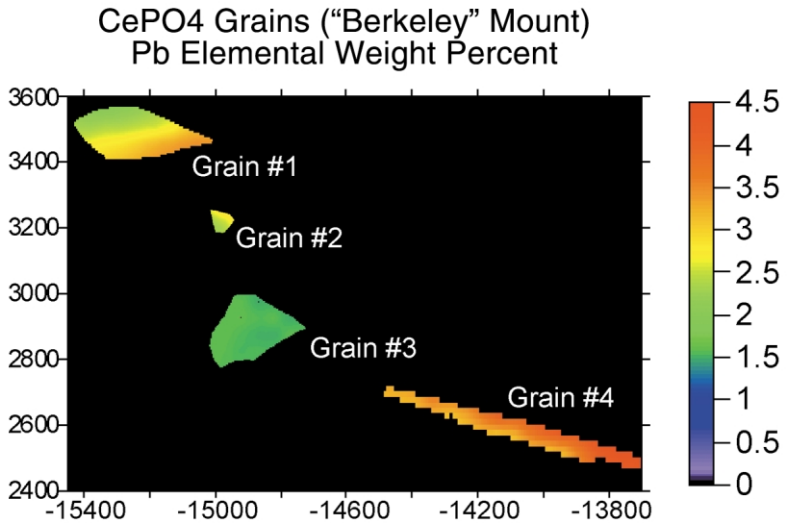

FIG. 5. Lead-distribution map in the four grains of $CePO_4$ mounted in the "Berkeley" *REE* standard block. Color scale in in elemental weight percent of Pb. Stage coordinates are in micrometers. Notice not only the significant variation within the grains but also the even greater variation from grain to grain. See Table 6 for a numerical summary of the average and standard deviations of each grain.

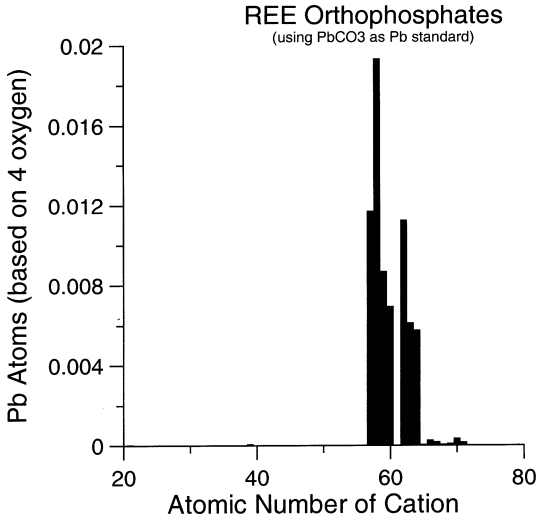

FIG. 6. Plot of Pb atoms per formula unit (based on 4 atoms of oxygen) *versus* atomic number of the cation. Element 61 (Pm) is unstable, and the orthophosphate was not produced at Oak Ridge. For all others, only the monoclinic forms for the orthophosphates were observably contaminated by the Pb flux used to dissolve the starting material prior to crystal growth. This contamination is likely present both as inclusions of flux and Pb incorporated into the crystal structure.

ACKNOWLEDGEMENTS

Thanks to Tim Teague at the UC Berkeley Petrographic Laboratory for his usual meticulous preparation of samples. William B. Simmons Jr. and Robert F. Martin provided helpful suggestions and corrections.

REFERENCES

ABRAHAM, M.M., BOATNER, L.A. & RAPPAZ, M. (1980): Novel measurement of hyperfine interactions in solids: $^{207}Pb^{3+}$ in YPO_4 and $LuPO_4$. *Phys. Rev. Lett.* **45**, 839-842.

BOATNER, L.A. & SALES, B.C. (1988): Monazite. *In* Radioactive Waste Forms for the Future (W. Lutze & R.C. Ewing, eds.). Elsevier, Amsterdam, The Netherlands (495-564).

DONOVAN, J.J., SNYDER, D.A. & RIVERS, M.L. (1993): An improved interference correction for trace element analysis. *Microbeam Analysis* **2**, 23-28.

DRAKE, M.J. & WEILL, D.F. (1972): New rare earth element standards for electron microprobe analysis. *Chem. Geol.* **10**, 179-181.

GOLDSTEIN, J.I., NEWBURY, D.E., ECHLIN, P., JOY, D.C., FIORI, C. & LIFSHIN, E. (1981): *Scanning Electron Microscopy and X-Ray Microanalysis*. Plenum, New York, N.Y.

JAROSEWICH, E. & BOATNER, L.A. (1991): Rare-earth element reference samples for electron microprobe analysis. *Geostandards Newsletter* **XV**, 397-399.

MILLIGAN, W.O, MULLICA, D.F., BEALL, G.W. & BOATNER, L.A. (1982): Structural investigations of YPO_4, $ScPO_4$ and $LuPO_4$. *Inorg. Chim. Acta* **60**, 39-43.

_____, _____, _____ & _____ (1983a): Structural investigations of $ErPO_4$, $TmPO_4$ and $YbPO_4$. *Acta Crystallogr.* **C39**, 23-24.

_____, _____, _____ & _____ (1983b): The structures of three lanthanide orthophosphates. *Inorg. Chim. Acta* **70**, 133-136.

_____, _____, PERKINS, H.O., BEALL, G.W. & BOATNER, L.A. (1983c): Crystal data for lanthanide orthophosphates with zircon-type structure. *Inorg. Chim. Acta* **77**, L23-25.

MULLICA, D.F, GROSSIE, D.A. & BOATNER, L.A. (1985a): Coordination geometry and structural determinations of $SmPO_4$, $EuPO_4$ and $GdPO_4$. *Inorg. Chim. Acta* **109**, 105-110.

_____, _____ & _____ (1985b): Structural refinements of praseodymium and neodymium orthophosphate. *J. Solid State Chem.* **58**, 71-77.

MONTEL, J.-M., FORET, S., VESCHAMBRE, M., NICOLLET, C. & PROVOST, A. (1996): Electron microprobe dating of monazite. *Chem. Geol.* **131**, 37-53.

NI, YUNXIANG, HUGHES, J.M. & MARIANO, A.N. (1995): Crystal chemistry of the monazite and xenotime structures. *Am. Mineral.* **80**, 21-26.

PARRISH, R.R. (1990): U–Pb dating of monazite and its application to geological problems. *Can. J. Earth Sci.* **27**, 1431-1450.

ROEDER, P.L. (1985): Electron-microprobe analysis of minerals for rare-earth elements: use of calculated peak-overlap corrections. *Can. Mineral.* **23**, 263-271.

_____, MACARTHUR, D., MA, XIN-PEI, PALMER, G.R. & MARIANO, A.N. (1987): Cathodoluminescence and microprobe study of rare-earth elements in apatite. *Am. Mineral.* **72**, 801-811.

SCOTT, V.D. & LOVE, G. (1983): *Quantitative Electron-Probe Microanalysis*. John Wiley & Sons, New York, N.Y.

SHANNON, R.D. (1976): Revised effective ionic radii and systematic studies of interatomic distances in halides and chalcogenides. *Acta Crystallogr.* **A32**, 751-767.

Received April 7, 2002, revised manuscript accepted December 1, 2002.